Formulation of 5D Edge Gyrokinetic Simulations*

X. Q. Xu,
Lawrence Livermore National Laboratory
University of California, Livermore, CA 94550

Presented at
Workshop on Long Time Simulations of Kinetic Plasmas
April 21, 2006; Dallas, TX

In collaboration with
Drs. Z. Xiong, B. I. Cohen, and R. H. Cohen,
M. R. Dorr, J. A. Hittinger, G. D. Kerbel, W. M. Nevins, and H. Qin

Acknowledgment to
Drs. Alain J. Brizard, J. Candy, P. Collela, L. Chen, A. Dimits, W. D Dorland,
T. S. Hahm, T. D. Rognlien, P. Snyder, M. V. Umansky, S. J. Wang, and W. X. Wang

*Performed for US DOE by LLNL under Contract W-7405-ENG-48 and is supported as LLNL LDRD project 04-SI-003.

Fully Nonlinear Ion gyrokinetic equations

Evolution of the plasma species is determined by coupled ion and electron kinetic equations for the time-dependent three-dimensional (5D) distribution functions simplified from H. Qin and et. al.(submitted to Contrib. Plasma Phys.; T. S. Hahm, Phys. Plasmas , Vol. 3, 4658 (1996). The gyrocenter distribution function $F_\alpha(\bar{\mathbf{x}}, \bar{\mu}, \bar{v}_\|, t)$ in gyrocenter coordinates: $Z \equiv (\bar{\mathbf{x}}, \bar{\mu}, E_0, t), \bar{\mathbf{x}} = \mathbf{x} - \rho, \rho = \mathbf{b} \times \mathbf{v}/\mathbf{\Omega_{ci}}$,

$$\frac{\partial F_\alpha}{\partial t} + \bar{\mathbf{v}}_\mathbf{d} \cdot \nabla_\perp F_\alpha + (\bar{v}_{\|\alpha} + v_{Banos}) \nabla_\| \partial F_\alpha + \left[q \frac{\partial \langle \Phi_0 \rangle}{\partial t} + \bar{\mu} \frac{\partial B}{\partial t} - \frac{qB}{B^*} \bar{v}_\| \nabla_\| \langle \delta\phi \rangle - q \mathbf{v}_\mathbf{d}^\mathbf{0} \cdot \bar{\nabla} \langle \delta\phi \rangle \right] \frac{\partial F_\alpha}{\partial E_0} = C(F_\alpha, F_\alpha),$$

$$\bar{\mathbf{v}}_\mathbf{d} = \frac{c\mathbf{b}}{qB_\|^*} \times \left(q \bar{\nabla} \langle \Phi \rangle + \bar{\mu} \bar{\nabla} B \right) + \bar{v}_\|^2 \frac{M_\alpha c}{qB_\|^*} (\bar{\nabla} \times \mathbf{b})$$

$$\bar{\mathbf{v}}_\mathbf{d}^\mathbf{0} = \frac{c\mathbf{b}}{qB_\|^*} \times \left(q \bar{\nabla} \langle \Phi_0 \rangle + \bar{\mu} \bar{\nabla} B \right) + \bar{v}_\|^2 \frac{M_\alpha c}{qB_\|^*} (\bar{\nabla} \times \mathbf{b})$$

$$\bar{v}_\| = \pm \sqrt{\frac{2}{M_\alpha} \left(E_0 - \bar{\mu} B - q \langle \Phi_0 \rangle \right)}, \qquad v_{Banos} = \frac{\mu c}{q} (\mathbf{b} \cdot \bar{\nabla} \times \mathbf{b}),$$

$$B_{\|\alpha}^* \equiv B \left[1 + \frac{\mathbf{b}}{\Omega_{c\alpha}} \cdot (v_\| \bar{\nabla} \times \mathbf{b}) \right], \Omega_{c\alpha} = \frac{qB}{M_\alpha c}, \mu = \frac{\mathbf{M}_\alpha \mathbf{v}_\perp^\mathbf{2}}{\mathbf{2B}}, \quad \langle \delta\phi \rangle = \langle \mathbf{\Phi} \rangle - \langle \mathbf{\Phi_0} \rangle.$$

Here $Z_\alpha e$, M_α are the electric charge and mass of electrons ($\alpha = e$), ions ($\alpha = i$). μ is the guiding center magnetic moment. The left-hand side of Eq. (1) describes the particle motion in the electric field and magnetic field. C_α is the Coulomb collision operator. The over-bar is used for the gyrocenter variables and $\langle \; \rangle$ denotes the gyroangle averaging. Here a splitting scheme has been used for the electric potential. The field Φ is split into two parts: Φ^0 is the large amplitude and the slow variation part; $\delta\phi$ is the small amplitude and the rapid variation part. E_0 is almost energy.

Gyrokinetic Poisson equation---Hong Qin

$$\nabla^2\phi(\mathbf{x}) = -4\pi\sum_s q_s\left[N + N_{\phi_0} + N_{\phi_1}\right],$$

$$N(\mathbf{x}) \equiv \int 2\pi w\,dw\,du\; I_0\left(\rho\nabla_\perp\right) F\left(\mathbf{x},w,u\right),$$

$$N_{\phi_0}(\mathbf{x}) \equiv \frac{1}{B_0^2}\left(\mathbf{e}_1\mathbf{e}_1+\mathbf{e}_2\mathbf{e}_2\right)\nabla\left[n(\mathbf{x})\left(\mathbf{D}+V_\parallel(\mathbf{x})\mathbf{b}\right)\cdot\nabla\mathbf{D}\right],$$

$$N_{\phi_1}(\mathbf{x}) \equiv -\phi_1(\mathbf{x})\sum_{i=1}^{\infty}\frac{2i}{(i!)^2}\left(\frac{\nabla_\perp^2}{4\Omega_0^2}\right)^i M_{2i-2}(\mathbf{x}) + \sum_{i,j=0}^{\infty}\frac{2(i+j)}{(i!j!)^2}\left(\frac{\nabla_\perp^2}{4\Omega_0^2}\right)^i\left[M_{2(i+j)-2}(\mathbf{x})\left(\frac{\nabla_\perp^2}{4\Omega_0^2}\right)^j\phi_1(\mathbf{x})\right],$$

Full FLR effect

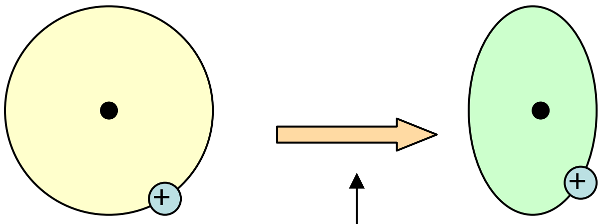

Orbit squeezing by large Er shear

$$n(\mathbf{x}) \equiv \int 2\pi w\,dw\,du\; F\left(\mathbf{x},w,u\right),$$

$$V_\parallel(\mathbf{x}) \equiv \frac{1}{n(\mathbf{x})}\int 2\pi w\,dw\,du\, F\left(\mathbf{x},w,u\right),$$

$$M_i(\mathbf{x}) \equiv \int 2\pi w\,dw\,du\; w^i F\left(\mathbf{x},w,u\right).$$

$$I_0\left(\rho\nabla_\perp\right) \equiv \sum_{i=0}^{\infty}\frac{1}{(i!)^2}\left(\frac{\nabla_\perp^2 w^2}{4\Omega_0^2}\right)^i$$

$F\left(\mathbf{x},w,u\right)$ -- total gyrocenter distribution function.

Evaluated at the particle coordinates.

Fully Nonlinear Gyro-kinetic Poisson equation in long wavelength limit

In the long wavelength limit $k_\perp \rho_\alpha \ll 1$, the self-consistent electrostatic potential are typically computed from the gyro-kinetic Poisson equation for the multiple species

$$\begin{aligned} \left(\sum_\alpha \frac{\rho_\alpha^2}{2\lambda_{D\alpha}^2}\right)\nabla_\perp^2\Phi &+ \left(\sum_\alpha \frac{\rho_\alpha^2}{2\lambda_{D\alpha}^2}\nabla_\perp \ln N_\alpha\right)\cdot\nabla_\perp\Phi + \nabla^2\Phi \\ &= -4\pi e\left[\sum_\alpha Z_\alpha N_\alpha(\mathbf{x},t) - n_e(\mathbf{x},t)\right] - \sum_\alpha \frac{\rho_\alpha^2}{2\lambda_{D\alpha}^2}\frac{1}{N_\alpha Z_\alpha e}\nabla_\perp^2 p_{\perp\alpha}. \end{aligned}$$

For the single species, the gyro-kinetic Poisson equation becomes

$$N_\alpha \nabla_\perp^2\Phi + \nabla_\perp\Phi\cdot\nabla_\perp N_\alpha + \frac{n_\alpha\lambda_{D\alpha}^2}{(\rho_\alpha^2/2)}\nabla^2\Phi = -\frac{1}{(\rho_\alpha^2/2)}\frac{T_{\perp\alpha}}{Z_\alpha^2 e}\left[Z_\alpha N_\alpha(\mathbf{x},t) - n_e(\mathbf{x},t)\right] - \frac{1}{Z_\alpha e}\nabla_\perp^2 p_{\perp\alpha}.$$

where the gyrocenter center density N_α and perpendicular ion pressure $p_{\perp\alpha}$ are defined by

$$\begin{aligned} N_\alpha(\mathbf{x},t) &\equiv \frac{2\pi}{M_\alpha}\int B_\parallel^* d\bar{v}_\parallel d\bar{\mu} F_\alpha, \\ n_e(\mathbf{x},t) &\equiv \frac{2\pi}{m_e}\int B_\parallel^* dv_\parallel d\mu f_e, \\ p_{\perp\alpha} &= \pi B\int dv_\parallel d\bar{\mu}(v_\perp^2 F_\alpha), \\ T_{\perp\alpha} &= \frac{p_{\perp\alpha}}{N_\alpha(\mathbf{x},t)} \end{aligned}$$

The n_α and $T_{\perp\alpha}$ are the normalization density and temperature. The ion gyroradius is $\rho_\alpha = \sqrt{2T_{\perp\alpha}/M_\alpha}/\Omega_\alpha$, the ion gyrofrequency is $\Omega_\alpha = Z_\alpha eB/M_\alpha c$, and the ion Debye length is $\lambda_{D\alpha}^2 = T_{\perp\alpha}/4\pi n_\alpha Z_\alpha^2 e^2$.

Fully Nonlinear Gyro-kinetic Poisson equation in arbitrary wavelength regime

In the arbitrary wavelength regime, the self-consistent electrostatic potential is computed from the gyro-kinetic Poisson equation:

$$0 = -4\pi e \left[\sum_\alpha Z_\alpha N_\alpha(\mathbf{x}, t) - n_e(\mathbf{x}, t) \right] - \sum_\alpha \frac{1}{\lambda_{D\alpha}^2} \left[\Gamma_0(b) - 1 \right] \Phi$$

where $\Gamma_0(b) = I_0(b)e^{-b}, b = \rho_\alpha^2 \nabla_\perp^2/2$, $I_0(b)$ is the usual zeroth-order modified Bessel function. The ion gyroradius is $\rho_\alpha = \sqrt{2T_{\perp\alpha}/M_\alpha}/\Omega_\alpha$, the ion gyrofrequency is $\Omega_\alpha = Z_\alpha eB/M_\alpha c$, and the ion Debye length is $\lambda_{D\alpha}^2 = T_{\perp\alpha}/4\pi N_\alpha Z_\alpha^2 e^2$. Here the dot product between the density and potential and the Debye shielding have been dropped for simplicity. The following first-order Padé approximation to Γ_0 is an excellent fit for $0 \le b \le 9$, and is therefore valid well into the typical ion gyrokinetic regime.

$$\Gamma(b) - 1 = \frac{b}{1-b}.$$

For single ion species, substituting a simple functional transformation

$$\Phi \;=\; \phi_L + \frac{T_{\perp\alpha}}{N_\alpha Z_\alpha^2 e} \left[Z_\alpha N_\alpha(\mathbf{x}, t) - n_e(\mathbf{x}, t) \right].$$

and Padé approximation Eq. (8) into Eq. (7) yields

$$\frac{\rho_\alpha^2}{2} \nabla_\perp^2 \phi_L \;=\; -\frac{T_\alpha}{N_\alpha Z_\alpha^2 e} \left[1 + \frac{\rho_\alpha^2}{2} \nabla_\perp^2 \ln\left(\frac{T_{\perp\alpha}}{N_\alpha} \right) \right] \left[Z_\alpha N_\alpha(\mathbf{x}, t) - n_e(\mathbf{x}, t) \right].$$

where ϕ_L can be solved using the gyrokinetic Poisson solver in the long wavelength limit.

Field-line-aligned coordinates

We choose field-line-aligned ballooning coordinates, $(x,\, y,\, z)$, which are related to the usual flux coordinates $(\psi,\, \theta,\, \zeta)$ by the relations

$$
\begin{aligned}
x &= \psi - \psi_s, \\
y &= \theta, \\
z &= \zeta - \int_{y_0}^{y} \nu(x,y)dy.
\end{aligned}
$$

as shown in Fig. 1. The covering area given by the square ABCD in the usual flux coordinates is the same as the parallelogram ABEF in the field-line-aligned coordinates. The magnetic separatrix is denoted by $\psi = \psi_s$. In this choice of coordinates, x is a flux surface label, y, the poloidal angle, is also the coordinate along the field line, and z is a field line label within the flux surface. In this coordinates the magnetic field has a Clebsch representation,

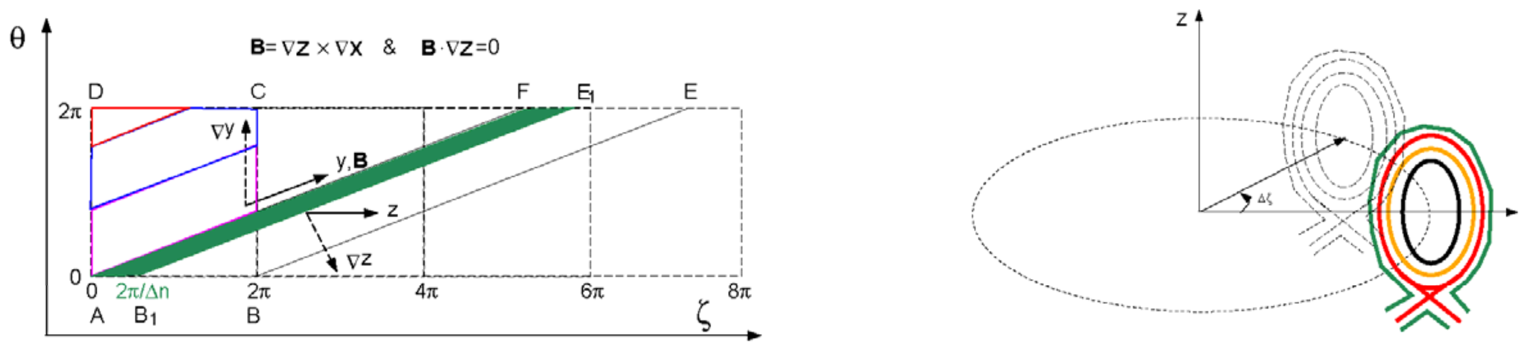

Figure 1: A sketch of the field-line-aligned coordinates mapping from (θ, ζ) to (y, z). The area covered by the square ABCD is for the usual flux coordinates $(\psi,\, \theta,\, \zeta)$. The area covered by parallelogram ABEF is for the field-line-aligned coordinates $(x,\, y,\, z)$. The green area covered by the parallelogram AB_1E_1F is a truncated simulation domain by the name of a annular toroidal wedge.

$$\mathbf{B} = \nabla z \times \nabla x.$$

Drift operator

The equilibrium total drift operator becomes

$$\begin{aligned}
\mathbf{v_{d0}} \cdot \nabla_\perp &= \frac{c}{qBB_\parallel^*}\left\{-\frac{I}{\mathcal{J}}\left[\left(\mu + \frac{M_\alpha v_\parallel^2}{B}\right)\frac{\partial B}{\partial y} + q\frac{\partial\langle\Phi_0\rangle}{\partial y}\right]\right\}\frac{\partial}{\partial\psi} \\
&+ \frac{c}{qBB_\parallel^*}\left\{\frac{I}{\mathcal{J}}\left[\left(\mu + \frac{M_\alpha v_\parallel^2}{B}\right)\frac{\partial B}{\partial x} + q\frac{\partial\langle\Phi_0\rangle}{\partial x}\right]\right\}\frac{\partial}{\partial\theta} \\
&- \frac{c}{qBB_\parallel^*}\left\{B_p^2\left[\left(\mu + \frac{M_\alpha v_\parallel^2}{B}\right)\frac{\partial B}{\partial x} + q\frac{\partial\langle\Phi_0\rangle}{\partial x}\right] + \frac{\mathcal{J}_{12}}{R^2}\left[\left(\mu + \frac{M_\alpha v_\parallel^2}{B}\right)\frac{\partial B}{\partial y} + q\frac{\partial\langle\Phi_0\rangle}{\partial y}\right]\right\}\frac{\partial}{\partial z}
\end{aligned}$$

The perturbed $\mathbf{E}\times\mathbf{B}$ drift operator becomes

$$\begin{aligned}
\delta\mathbf{v_d} \cdot \nabla_\perp &= \frac{c}{BB_\parallel^*}\left\{-\frac{I}{J}\frac{\partial\langle\delta\phi\rangle}{\partial\theta} + B_p^2\frac{\partial\langle\delta\phi\rangle}{\partial z}\right\}\frac{\partial}{\partial\psi} \\
&+ \frac{c}{BB_\parallel^*}\left\{\frac{I}{\mathcal{J}}\frac{\partial\langle\delta\phi\rangle}{\partial\psi} + \frac{\mathcal{J}_{12}}{R^2}\frac{\partial\langle\delta\phi\rangle}{\partial z}\right\}\frac{\partial}{\partial\theta} \\
&- \frac{c}{BB_\parallel^*}\left\{B_p^2\frac{\partial\langle\delta\phi\rangle}{\partial\psi} + \frac{\mathcal{J}_{12}}{R^2}\frac{\partial\langle\delta\phi\rangle}{\partial\theta}\right\}\frac{\partial}{\partial z},
\end{aligned}$$

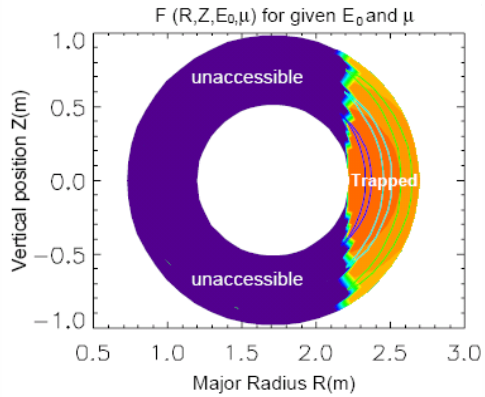

when the conventional turbulence ordering ($k_\parallel \ll k_\perp$) is used, the perturbed $\mathbf{E}\times\mathbf{B}$ drift operator can be further reduced to a simple form

$$\delta\mathbf{v_d} \cdot \nabla_\perp = \frac{cB}{B_\parallel^*}\left(\frac{\partial\langle\delta\phi\rangle}{\partial z}\frac{\partial}{\partial x} - \frac{\partial\langle\delta\phi\rangle}{\partial x}\frac{\partial}{\partial z}\right)$$

where $\partial/\partial\theta \simeq -\nu\partial/\partial z$ is used.

The general perpendicular Laplacian operator

We use the general perpendicular Laplacian operator

$$
\begin{aligned}
\mathcal{J}\nabla_\perp^2\Phi &= \frac{\partial}{\partial x}\left(\mathcal{J}\mathcal{J}_{11}\frac{\partial\Phi}{\partial x} + \mathcal{J}\mathcal{J}_{12}\frac{\partial\Phi}{\partial y} + \mathcal{J}\mathcal{J}_{13}\frac{\partial\Phi}{\partial z}\right) \\
&+ \frac{\partial}{\partial y}\left(\mathcal{J}\mathcal{J}_{21}\frac{\partial\Phi}{\partial x} + \mathcal{J}\mathcal{J}_{22}\frac{\partial\Phi}{\partial y} + \mathcal{J}\mathcal{J}_{23}\frac{\partial\Phi}{\partial z}\right) \\
&+ \frac{\partial}{\partial z}\left(\mathcal{J}\mathcal{J}_{31}\frac{\partial\Phi}{\partial x} + \mathcal{J}\mathcal{J}_{32}\frac{\partial\Phi}{\partial y} + \mathcal{J}\mathcal{J}_{33}\frac{\partial\Phi}{\partial z}\right) \\
&- \left(\frac{B_p}{hB}\right)\frac{\partial}{\partial y}\left[\left(\frac{B_p}{hB}\right)\frac{\partial\Phi}{\partial y}\right] - \left(\frac{B_p}{hB}\right)^2\frac{\partial\ln B}{\partial y}\frac{\partial\Phi}{\partial y}.
\end{aligned}
$$

The general perpendicular Laplacian operator for axisymmetric potential $\Phi_0(x,y)$ is

$$
\begin{aligned}
\mathcal{J}\nabla_\perp^2\Phi_0 &= \frac{\partial}{\partial x}\left(\mathcal{J}\mathcal{J}_{11}\frac{\partial\Phi_0}{\partial x} + \mathcal{J}\mathcal{J}_{12}\frac{\partial\Phi_0}{\partial y}\right) \\
&+ \frac{\partial}{\partial y}\left(\mathcal{J}\mathcal{J}_{21}\frac{\partial\Phi_0}{\partial x} + \mathcal{J}\mathcal{J}_{22}\frac{\partial\Phi_0}{\partial y}\right) \\
&- \left(\frac{B_p}{hB}\right)\frac{\partial}{\partial y}\left[\left(\frac{B_p}{hB}\right)\frac{\partial\Phi_0}{\partial y}\right] - \left(\frac{B_p}{hB}\right)^2\frac{\partial\ln B}{\partial y}\frac{\partial\Phi}{\partial y}.
\end{aligned}
$$

For the perturbed potential $\delta\phi$, if we drop $\delta/\delta y$ terms due to the elongated nature of the turbulence ($k_{||}/k_\perp \ll 1$), we obtain

$$
\mathcal{J}\nabla_\perp^2\delta\phi = \frac{\partial}{\partial x}\left(\mathcal{J}\mathcal{J}_{11}\frac{\partial\delta\phi}{\partial x} + \mathcal{J}\mathcal{J}_{13}\frac{\partial\delta\phi}{\partial z}\right) + \frac{\partial}{\partial z}\left(\mathcal{J}\mathcal{J}_{31}\frac{\partial\delta\phi}{\partial x} + \mathcal{J}\mathcal{J}_{33}\frac{\partial\delta\phi}{\partial z}\right).
$$

In this formulation, we keep the poloidal variation of the zonal flow $\Phi_0(\psi,\theta)$.

Boundary Conditions — Radial (x)

Radial (x) boundary condition for potential Φ

Use the neoclassical analytical ambipolar value E_r as the boundary condition at core boundary surface

$$E_\psi|^{\psi_c} = E_\psi^{neo} = \frac{B}{cRB_t}\langle U_{\alpha\|}\rangle - \frac{T_\alpha}{Z_\alpha e}\left\{k\frac{\partial \ln T_\alpha}{\partial\psi} - \frac{\partial \ln P_\alpha}{\partial\psi}\right\} \tag{19}$$

$$\alpha_b\Phi|^{\psi_{c,w}} + (1-\alpha_b)\frac{\partial\Phi}{\partial\psi}|^{\psi_{c,w}} = \alpha_a. \tag{20}$$

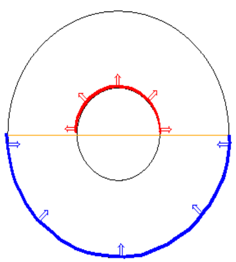

Radial (x) boundary condition for distribution function F

The radial Robin boundary condition at the inner core surface $\psi = \psi_c$ and the outer wall surface $\psi = \psi_w$:

$$C_{br}F_{b\alpha}|^{\psi_c,\psi_w} + (1-C_{br})\frac{\partial F_{b\alpha}}{\partial r}|^{\psi_c,\psi_w} = \left[C_{br} - (1-C_{br})\frac{\Gamma_{b\alpha}}{D_{b\alpha}n_{b\alpha}}\right]F_{mb\alpha}. \tag{21}$$

$$F_{mb\alpha} = \frac{n_{b\alpha}}{(\sqrt{\pi}v_{thb\alpha})^3\mathcal{F}_0}\exp\left[-\frac{\mu B}{T_{b\alpha}} - \frac{(v_\| - u_{b\alpha})^2}{v_{thb\alpha}^2}\right]. \tag{22}$$

This is a generalization of the Dirichlet ($C_{br} = 1$) and Neumann ($C_{br} = 0$) boundary conditions.

Sheath boundary conditions in SOL and private flux regions

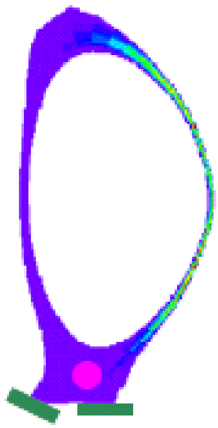

Sheath boundary conditions for potential Φ

If both electron and ion are kinetic, the sheath potential is determined:

$$\Gamma_{i,sh} = \frac{2\pi B}{M_\alpha^2}\int_0^\infty dE_0 \int_0^{E_0 - Z_\alpha e\Phi_{sh}} \frac{d\mu}{|v_\parallel|} v_\parallel F_i^\sigma, \quad (27)$$

$$\Gamma_{e,sh} = \frac{2\pi B}{m_e^2}\int_{e\Phi_{sh}}^\infty dE_0 \int_0^{E_0 + e\Phi_{sh}} \frac{d\mu}{|v_\parallel|} v_\parallel F_e^\sigma, \quad (28)$$

$$\Gamma_{i,sh} = \Gamma_{e,sh}. \quad (29)$$

where there is an energetic group of impinging electrons that overcome the potential barrier and reach the wall with the energy $E_0 > e\Phi_{sh}$.

Sheath boundary conditions for distribution function F

If both electron and ion are kinetic, the electron distribution function is:

$$F_\alpha(\psi,\theta,\zeta,E_0,\mu) = \begin{cases} F_\alpha(\psi,\theta,\zeta,E_0,\mu), & v_\parallel \geq 0 \\ 0, & v_\parallel \leq 0 \end{cases} \quad (30)$$

$$f_e(\psi,\theta,\zeta,E_0,\mu) = \begin{cases} f_e(\psi,\theta,\zeta,E_0,\mu), & |v_\parallel| \leq v_{SH} \;\; if \;\; v_\parallel \leq 0 \;\; or \;\; v_\parallel \geq 0 \\ 0, & |v_\parallel| \geq v_{SH} \;\; if \;\; v_\parallel \leq 0 \end{cases} \quad (31)$$

where the impinging ions are not confined for the perfectly absorbing wall and the current through the sheath is zero with no biasing. A convention regarding the sign of the parallel velocity is that it is considered positive if it has a positive projection on θ axis. Here the positive θ axis is pointing to the plate/wall. where there is an energetic group of impinging electrons that overcome the potential barrier, reach the wall with the energy $E_0 > e\Phi_{sh}$, and lost. Here $v_{SH} = \sqrt{2e\Delta\Phi_{SH}/m_e}$, $\Delta\Phi_{SH}$ is the sheath potential.

Tempest exhibits collisionless damping of GAMs and zonal Flow

- **Axis-symmetric mode (no toroidal variation)**
  - **– Parallel ion dynamics**
  - **– Magnetic curvature**
  - **– Acceleration (Nonlinear Landau damping)**
  - **➔ TEMPEST should see GAMs**
- **Tempest model**
  - **Drift kinetic ions with radial drift, streaming, and acceleration**
  - **Boltzmann electron**
  - **Gyrokinetic Poisson equation in limit small ρ_s/L_x**
  - **Dirichlet radial boundary conditions**
- **GAMs provide opportunity to "verify" TEMPEST physics**
  - **Rosenbluth-Hinton residual**

$$\frac{\phi(t=\infty)}{\phi(t=0)} \approx \frac{1}{1+1.6q^2/\sqrt{\varepsilon}}$$

  - **Frequency**

$$\omega_{GAM} \approx \sqrt{\frac{7}{8}}\frac{v_{Ti}}{R}$$

$\phi(t)/\phi(t=0)$

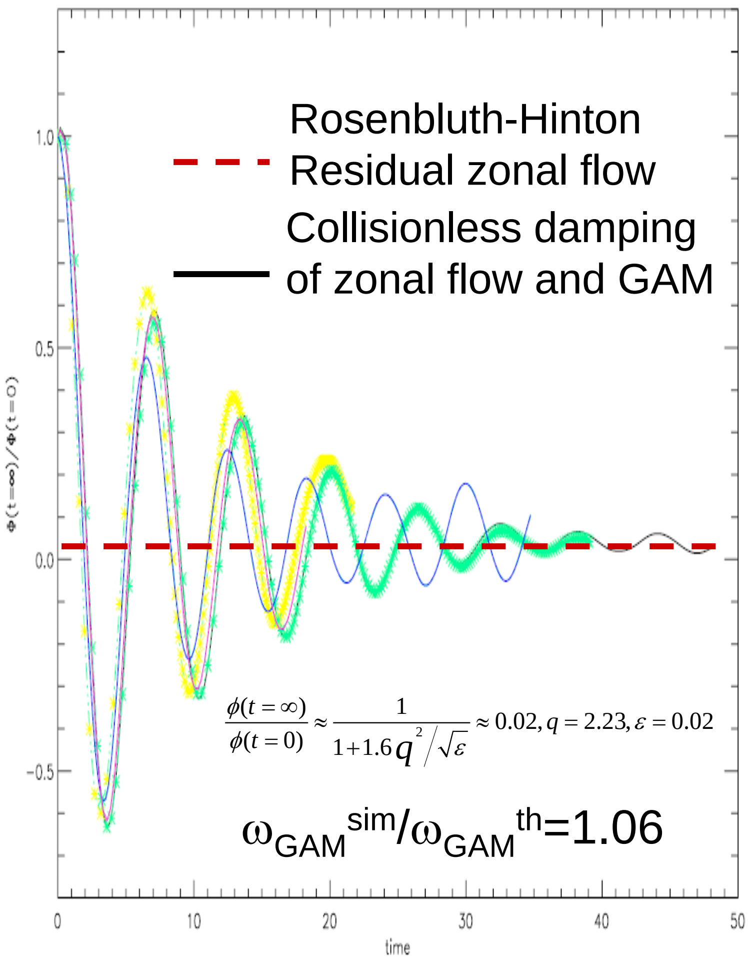

Time(v_{ti}/R_0)

Tempest exhibits collisionless damping of GAMs and zonal Flow

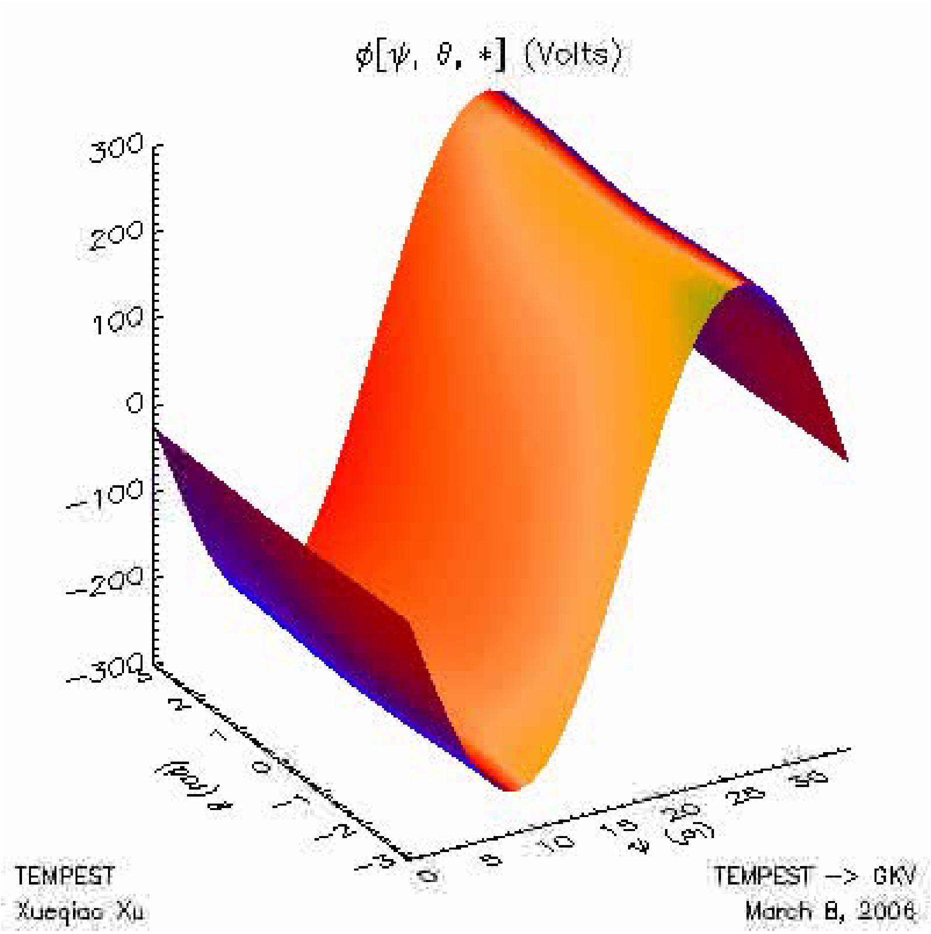

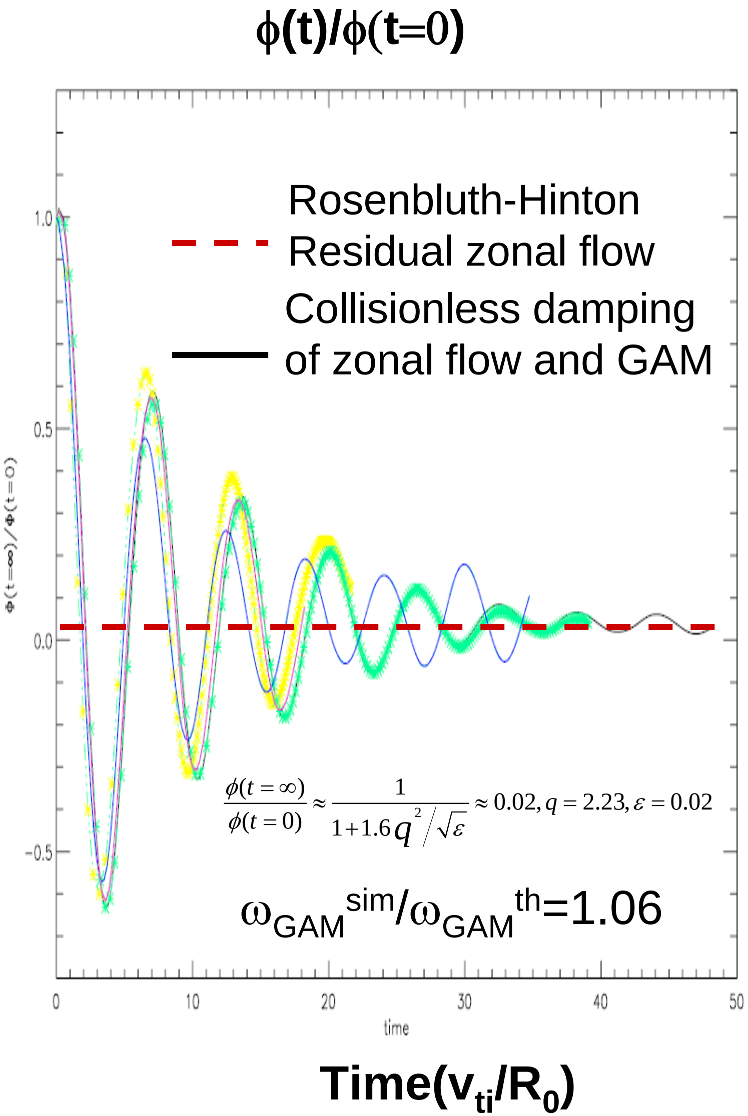

GAMs simulations converge with n_v, n_θ, and K_{Emax}

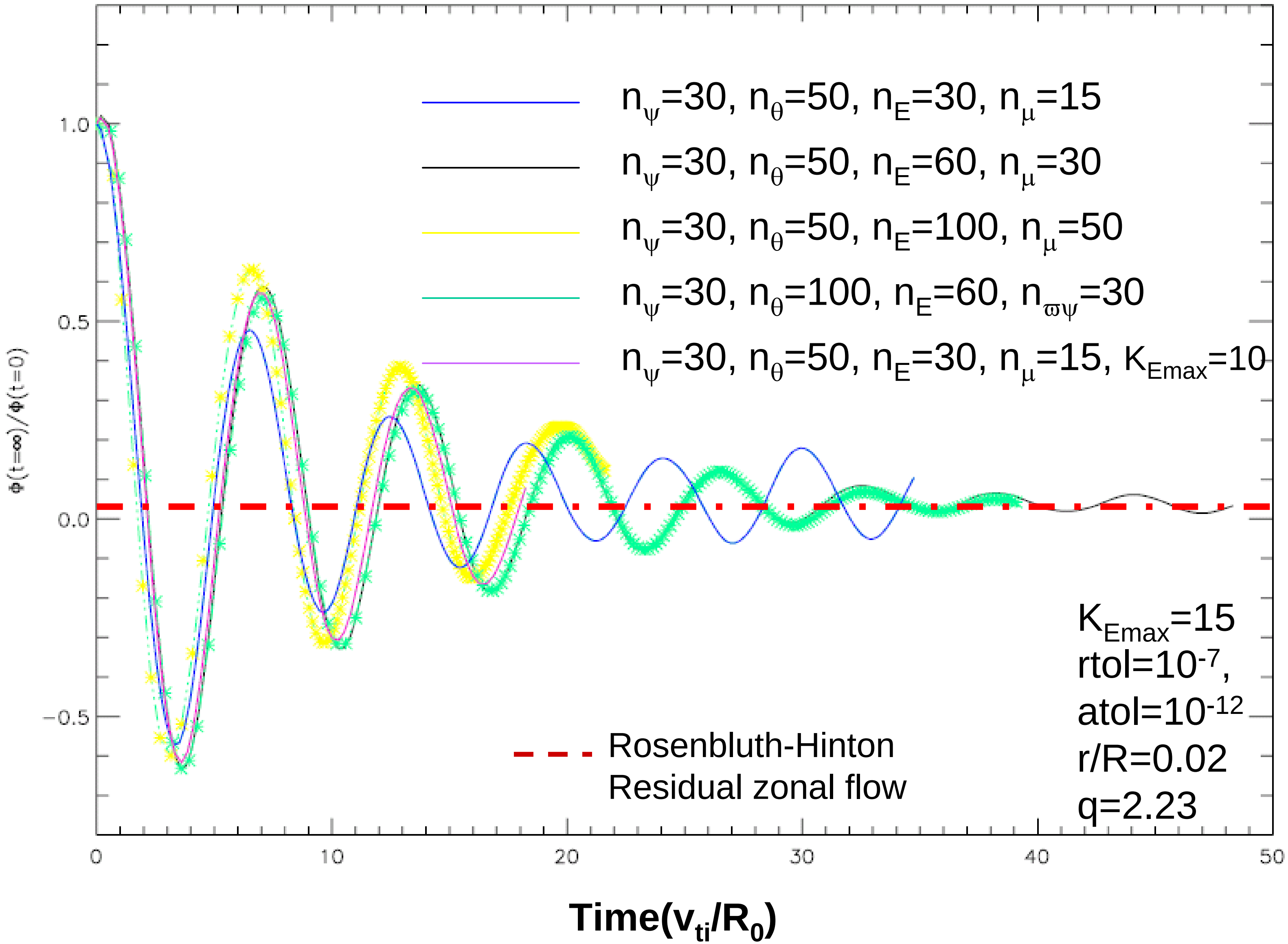

GAMs simulations converge with n_v and n_θ

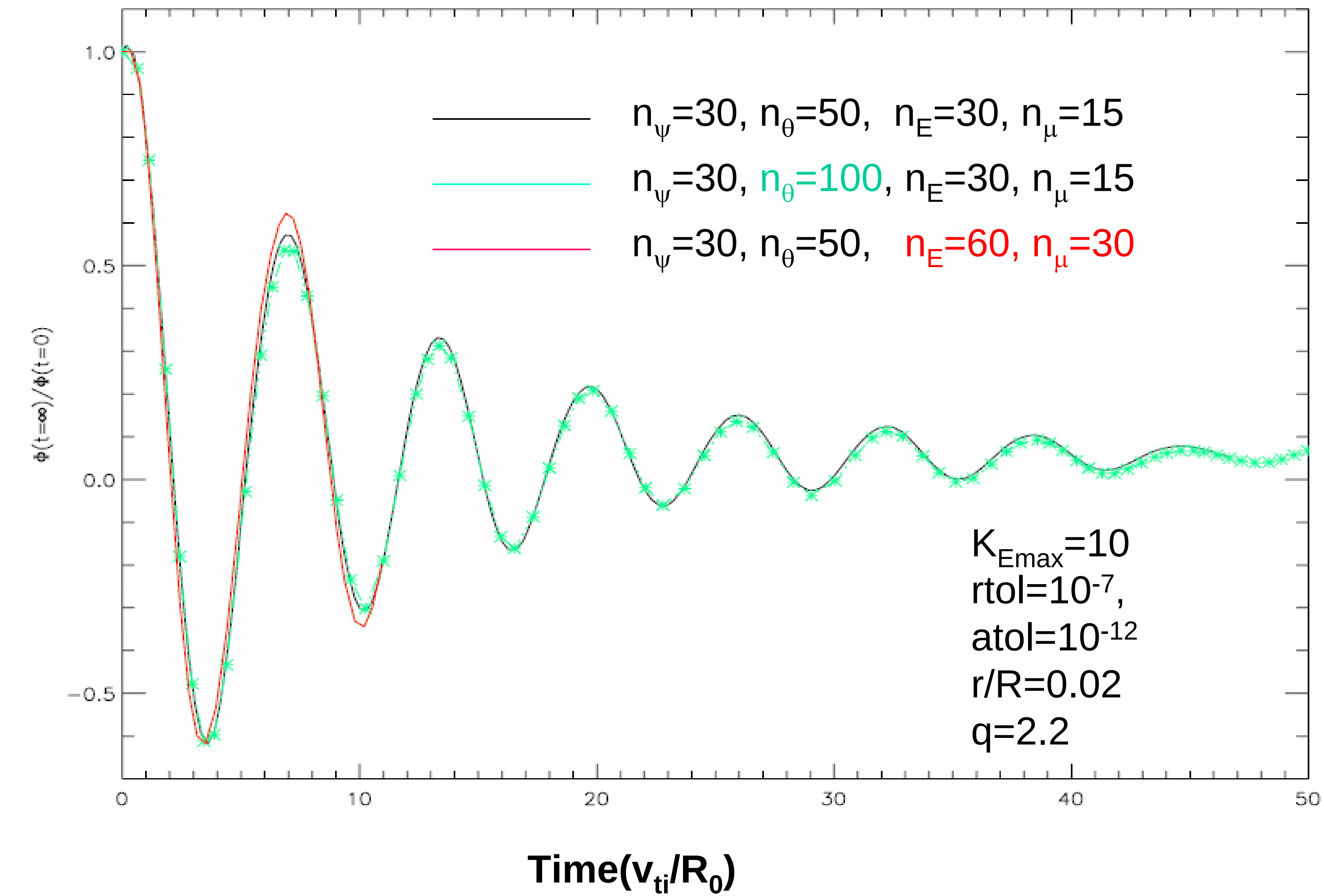

Maximum kinetic energy has to be 10x thermal energy

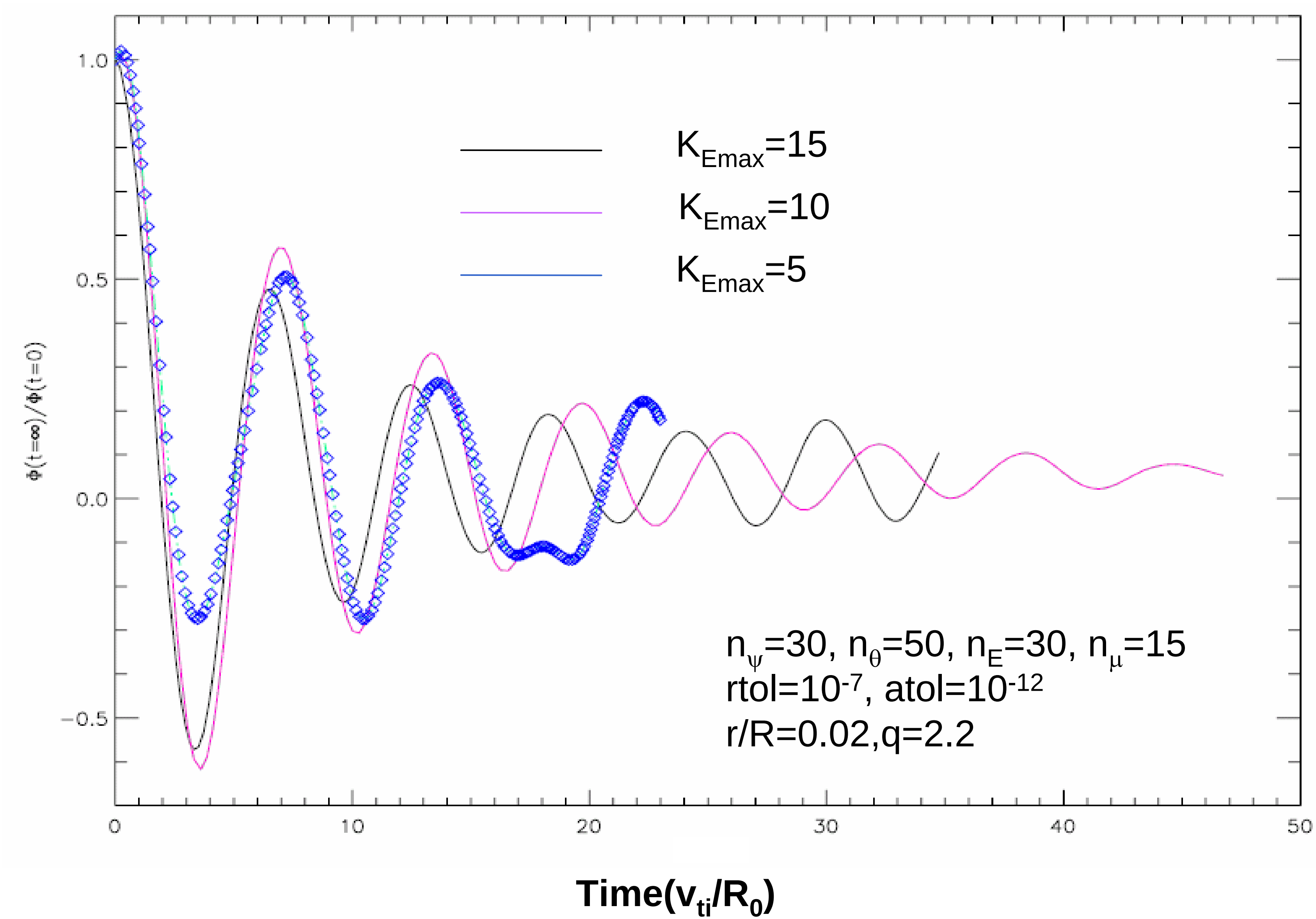

Contour plot of distribution function

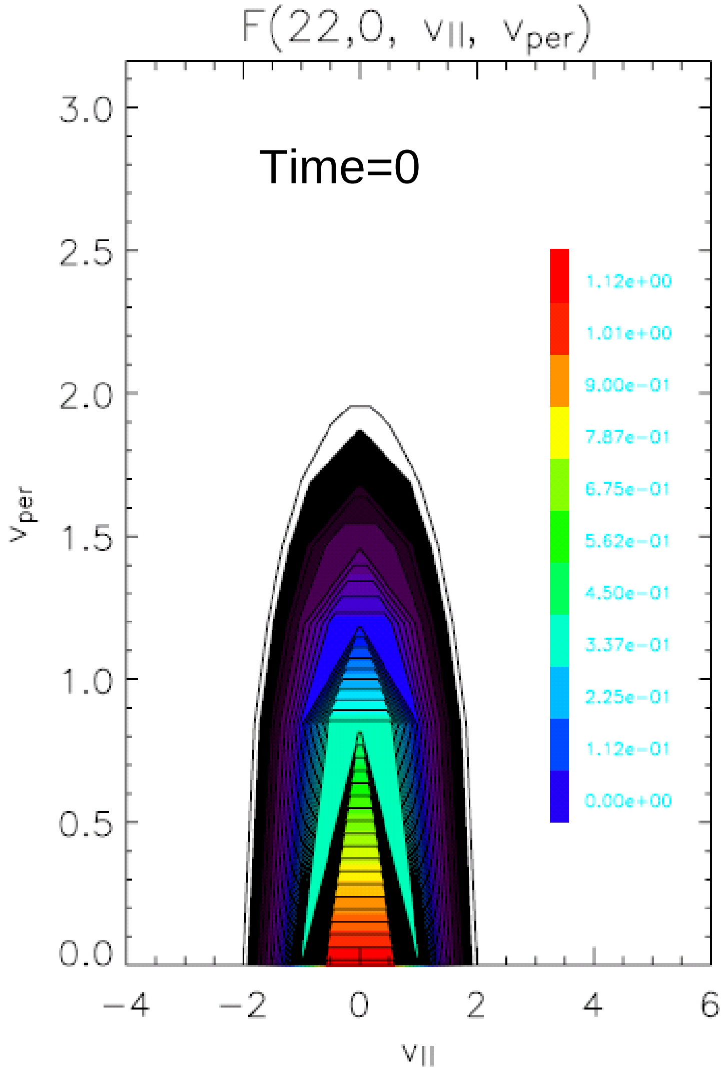

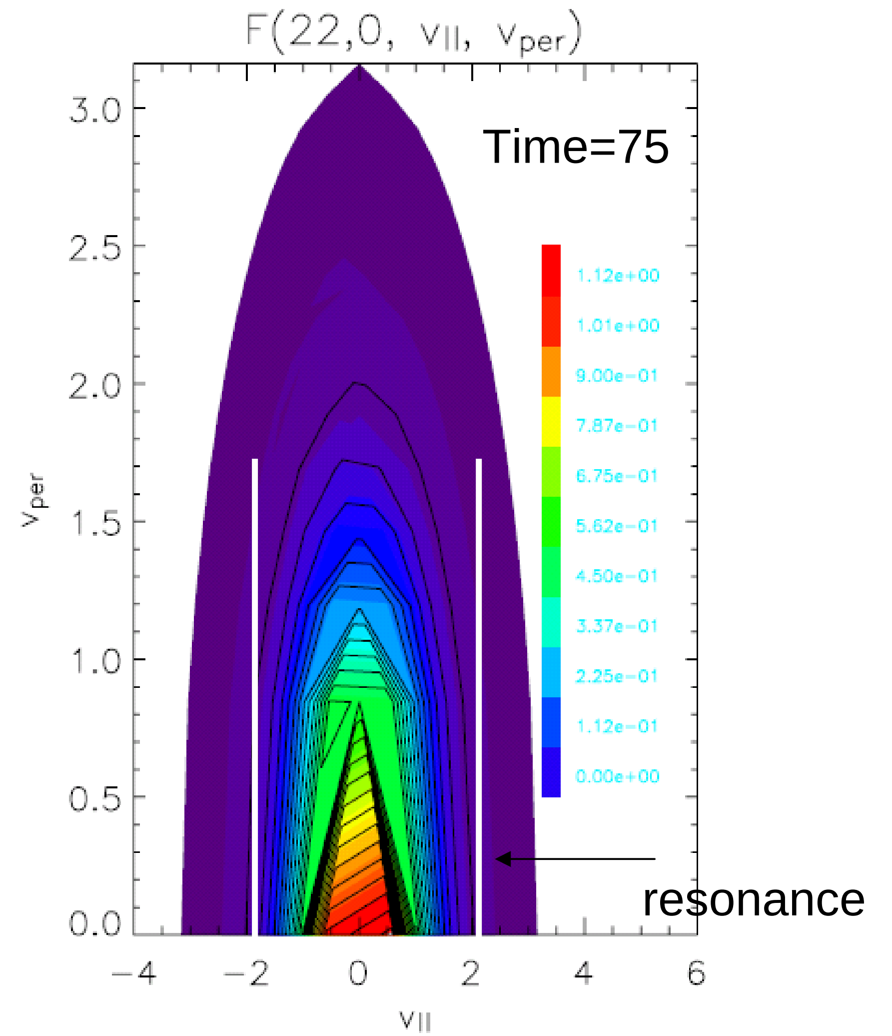

5D development plan

- Completed formulation of 5D gyrokinetic simulation model
  - A basic set of equations
    - Electrostatic turbulence
    - Arbitrary wavelength limit
  - Choice of coordinate system
    - Field-aligned coordinates
- Planned numerical implementation
  - Implementing special processor scheduling for 5D data communication
  - Designing dual coordinate sets for radial difference
  - Adding toroidal drift
    - Change the 2D spatial loop to 3D
    - Add toroidal convection
  - Extend field solve to 3D
  - Developing gyroaverging module
- Defined benchmark test problems
  - ITG turbulence
    - Rosenbluth-Hinton zonal flow residual
    - Linear growth rates of ITG modes
  - Drift wave turbulence